Theoret. Chim. Acta (Berl.) 32, 111—134 (1973)

An Intermediate Neglect of Differential Overlap Technique for Spectroscopy: Pyrrole and the Azines

J. Ridley and Michael Zerner

Department of Chemistry, University of Guelph, Guelph, Ontario NIG 2WI, Canada

Received May 9, 1973

An LCAO-MO-SCF-CI model along the lines introduced by Del Bene and Jaffé is developed that is capable of reproducing the better identified observed spectra of nitrogen heterocycles with a rms error of $\sim 1000\,\mathrm{cm}^{-1}$. The model is applied to the spectra of pyrrole, benzene, pyridine, the diazines, symmetric triazine and symmetric tetrazine. The benzene and pyridine spectra are reproduced nearly exactly. The band observed in pyrrole at ~ 6.5 eV is calculated as two bands at ~ 6.5 eV, but they are assigned $\pi \rightarrow \sigma^*$ and not $\pi \rightarrow \pi^*$. No evidence is found for the low lying ${}^1B_{2g}$ in pyrazine, reported at $\sim 30400\,\mathrm{cm}^{-1}$ in pure crystals. The lowest excited singlet of sym. triazine is calculated as ${}^1E''$ $(n \rightarrow \pi^*)$, not ${}^1A_2''$ $(n \rightarrow \pi)$, in agreement with a recent interpretation of Fischer and Small. Several bands are reassigned, and the electronic nature of the transitions discussed. Naphthalene and quinoxaline are examined to insure that no large drift of results are met with molecules of other sizes. Comparison of eigenvalues with molecular ionization potentials is made. Here the numerical agreement appears satisfactory for the first few ionization potentials only.

Key words: Spectroscopic INDO – Benzene – Pyrrole – Pyridine – Azines

Introduction

The purpose of this work is to examine the spectra of nitrogen containing heterocycles. Although the molecules of initial interest were of somewhat more ambitious size than those reported here, it was discovered that none of the quantum mechanical models available did an accurate job on smaller molecules, and that many interesting experimental uncertanties still existed in the spectra of pyrrole and the azines.

The first part of this paper develops a quantum mechanical model which seems to be capable of reproducing the observed singlet spectra of the compounds studied with a rms error of approximately $1000\,\mathrm{cm}^{-1}$: the second applies the method to the spectra of pyrrole, benzene, pyridine, the diazines, symmetric triazine and symmetric tetrazine. To insure that there is no systematic drift in the accuracy of the method with molecular size and shape we also report results on naphthalene and quinoxaline.

The Model

a) INDO/1

Considerable success has been met in organizing the $\pi \rightarrow \pi^*$ spectra of aromatic compounds utilizing the Pariser-Parr-Pople SCF CI model [1]. Extensions of this method to incorporate lone pairs and inductive effects, still basically within the *pi* electron framework have increased accuracy and allowed a rudimentary analysis of $n \rightarrow \pi^*$ transitions [2]. With the introduction of approximate all valence methods of rapid execution, models which automatically introduce the polarizability of the core, as well as extending consideration to all low lying excitations became readily available. Perhaps the most appropriate model to employ is the Complete Neglect of Differential Overlap (CNDO) or Intermediate Neglect of Differential Overlap (INDO) method of Pople and coworkers [3, 4], as aspects of the Pariser-Parr-Pople model responsible for its successes in explaining $\pi \rightarrow \pi^*$ spectra are systematically incorporated. Toward the goal of describing spectra Del Bene and Jaffé reparameterized CNDO/2 [5] and were able to reproduce many of the spectral features of nitrogen containing compounds, although with considerable less accuracy than we desired. Nevertheless, their initial success stimulated us to believe that the basic method could be called upon for more accuracy and greater detail.

The method we employ is a modification of INDO. We chose INDO over CNDO as the former includes the one-center exchange integrals necessary in accurately separating different terms from within a configuration. (For example, the singlet and triplet arising from $n \rightarrow \pi^*$ transitions are degenerate within the CNDO approximation). In addition, we have found that these integrals increase the interaction between states arising from $\pi \rightarrow \pi^*$ and $\sigma \rightarrow \sigma^*$ transitions, in many cases reducing the calculated transition energies and oscillator strengths.

"INDO/1" is used in this study in preference to "INDO/2". The former refers to a technique in which the one-center core integrals, $U_{\mu\mu}$, are obtained from ionization potentials only (as in CNDO/1), but the evaluation of nuclear attraction integrals is retained as $V_{AB} = Z_A \gamma_{AB}$ (as in CNDO/2), where γ_{AB} is the appropriate two-center Coulomb integral between atoms A and B.

The choice of one-center core integrals from ionization potentials, rather than from ionization potentials and electron affinities, is supported in several ways. Electron affinities for many valence states of many atoms are not accurately known. Secondly, the calculations which relate minimum basis sets to negative ions without orbital expansions are less accurate than such calculations on corresponding neutral and positive ions (using Slater's exponents [6] for neutral atoms). This fact sheds some doubt on the validity of the equations relating minimum basis set calculations to electron affinities. Thirdly, *ab-initio* calculations, properly core-orthogonalized, and then symmetrically orthogonalized more closely resemble INDO calculations with parameters only from ionization potentials [7]. Finally, spectroscopic results are improved.

The approximation $V_{AB} = Z_A \gamma_{AB}$ is sound, as it compensates for errors introduced by assuming an orthogonal basis set (and thus Zero Differential Overlap), while in practice employing a basis set of non-orthogonal Slater functions [3c]. For the core integrals, assuming the exponent of an s orbital is equal to that of the p, we derive

$$\begin{aligned} U_{\mu\mu} &\equiv \left(\mu\middle| -1/2\nabla^2 - \frac{Z_A}{R_A} + V\middle|\mu\right) \\ &= I_\mu - (Z_A - 1)F^0(ss) + 1/6m\,G^1(sp) && s \text{ a.o.} \\ &= I_\mu - (Z_A - 1)F^0(ss) + 1/6lG^1(sp) + \frac{2}{25}(m-1)F^2(pp) && p \text{ a.o.} \end{aligned}$$

where orbital μ is centered on atom A, V is a pseudo-potential accomodating the neglected inner shells, and I_μ, the ionization potential for the process $s^l p^m \rightarrow s^{l-1} p^m + (s)$ or $s^l p^m \rightarrow s^l p^{m-1} + (p)$. Table 1 gives the values of the ionization potentials and Slater-Condon Factors ($G^1(sp)$ and $F^2(pp)$) that we use. These are obtained from the atomic spectral tables of Moore [8] in a straight-forward fashion [9].

The INDO method is now summarized for a closed shell configuration as:

$$\begin{aligned}
&\boldsymbol{F}\boldsymbol{C}_a = \varepsilon_a \boldsymbol{C}_a \\
&F_{\mu\mu} = U_{\mu\mu} + \sum_{\sigma}^{A} P_{\sigma\sigma}[(\mu\mu|\sigma\sigma) - 1/2(\mu\sigma|\mu\sigma)] + \sum_{B \neq A} (P_{BB} - Z_B)\gamma_{AB} \qquad \mu \in A \\
&F_{\mu\nu} = 3/2 P_{\mu\nu}(\mu\nu|\mu\nu) - 1/2 P_{\mu\nu}(\mu\mu|\nu\nu), \qquad \mu, \nu \in A \\
&F_{\mu\nu} = \bar{S}_{\mu\nu}(\beta_A + \beta_B)/2 - P_{\mu\nu}\gamma_{AB}/2, \qquad \mu \in A, \nu \in B \\
&P_{\mu\nu} = 2 \sum_{a}^{\text{m.o.}} C_{\mu a} C_{\nu a} \\
&P_{AA} = \sum_{\mu}^{A} P_{\mu\mu} \\
&(\mu\nu|\sigma\lambda) = \int d\tau_1 d\tau_2 \chi_\mu^*(1)\chi_\nu(1) \frac{1}{r_{12}} \chi_\sigma^*(2)\chi_\lambda(2) \\
&\gamma_{AB} = (\bar{\mu}\bar{\mu}|\bar{\nu}\bar{\nu}), \qquad \mu \in A, \nu \in B
\end{aligned} \tag{2}$$

In the above, $\boldsymbol{F}$ is the Fock matrix, $\boldsymbol{C}_a$ the coefficients of molecular orbital a, ε_a, the m.o. eigenvalues, $\boldsymbol{P}$, the first order density (the charge and bond order matrix in the orthogonal set), and $\bar{\mu}$ is the μ'th a.o. treated as if it were of s symmetry.

For first row atoms five types of one center integrals are encountered, and they are treated in an exact fashion, but from the semi-empirical Slater Condon factors of Table 1.

$$\begin{aligned}
(ss|ss) &= (ss|pp) = F^0 \\
(sp|sp) &= \frac{1}{3} G^1(sp) \\
(p_x p_x|p_x p_x) &= F^0(pp) + \frac{4}{25} F^2(pp) \\
(p_x p_x|p_y p_y) &= F^0(pp) - \frac{2}{25} F^2(pp) \\
(p_x p_y|p_x p_y) &= \frac{3}{25} F^2(pp).
\end{aligned} \tag{3}$$

For further details of the INDO technique, its rationale and its successes, one is referred to the original work of Pople, Beveridge and Dobosh [4].

b) Calculation of Spectra

The calculation consists of two parts. The first of these is the calculation of the ground state yielding molecular orbital coefficients and eigenvalues. The ground state calculation is then followed by a configuration interaction calculation.

In all cases studied, the ground state is closed-shell (singlet). Those molecular orbitals which do not have electrons assigned to them (virtual orbitals) are used to generate the "pure" configurations.

Excitation of an electron from a filled orbital "i" to a virtual orbital "a" gives rise to a singlet and a triplet configuration. The energy corresponding to a singlet-singlet transition between pure configurations is given by:

$$\Delta E_{ia} = \varepsilon_a - \varepsilon_i - J_{ia} + 2K_{ia} \tag{4}$$

where ε_i and ε_a are the orbital energies of orbitals i and a respectively; J_{ia} is the molecular Coulomb integral:

$$\begin{aligned} J_{ia} &= \int \phi_i^*(1)\phi_i(1)\phi_a^*(2)\phi_a(2)\frac{1}{r_{12}}\,d\tau_1 d\tau_2 \\ &= (ii|aa)\,; \end{aligned} \tag{5}$$

and K_{ia} is the molecular exchange integral:

$$\begin{aligned} K_{ia} &= \int \phi_i^*(1)\phi_a(1)\phi_a^*(2)\phi_i(2)\frac{1}{r_{12}}\,d\tau_1 d\tau_2 \\ &= (ia|ai)\,. \end{aligned} \tag{6}$$

The corresponding expression for the singlet-triplet energy is:

$$\Delta E_{ia} = \varepsilon_a - \varepsilon_i - J_{ia}\,. \tag{7}$$

Under the CNDO approximation the integrals

$$\begin{aligned} (ij|kl) &= \int \phi_i^*(1)\phi_j(1)\phi_k^*(2)\phi_l(2)\frac{1}{r_{12}}\,d\tau_1 d\tau_2 \\ &= \sum_{\alpha\beta\gamma\delta} C_{i\alpha}C_{j\beta}C_{k\gamma}C_{l\delta}(\alpha\beta|\gamma\delta) \end{aligned} \tag{8}$$

(where the indices i, j, k, l refer to molecular orbitals; the $\alpha, \beta, \gamma, \delta$, refer to atomic orbitals) reduce to:

$$(ij|kl)_{\mathrm{CNDO}} = \sum_{\alpha\gamma} C_{i\alpha}C_{j\alpha}C_{k\gamma}C_{l\gamma}\gamma_{\alpha\gamma}\,. \tag{9}$$

This term is equal to zero when α and γ are a *pi* and a sigma orbital respectively.

Under the INDO approximation many terms of Eq. (8) do not reduce to zero, as indeed they should not. We obtain:

$$\begin{aligned}(ij|kl) = &\sum_{\substack{\alpha\neq\beta\\ \gamma\neq\delta}} C_{i\alpha}C_{j\beta}C_{k\gamma}C_{l\delta}(\alpha\beta|\gamma\delta)\delta^{AB}\delta^{CD}\delta^{AC}\\ &+\sum_{\alpha\gamma} C_{i\alpha}C_{j\alpha}C_{k\gamma}C_{l\gamma}\delta^{AC}\Delta_{\alpha\gamma}+(ij|kl)_{\mathrm{CNDO}} \qquad (10)\\ &\alpha\in A,\ \beta\in B,\ \gamma\in C,\ \delta\in D\\ \Delta_{\alpha\gamma}\equiv\ &(\alpha\alpha|\gamma\gamma)-F^0(\alpha\gamma)\,.\end{aligned}$$

The first term refers to the situation when α, β, γ and δ are all on one center; the second term refers to the situation when α and γ are on the same center. An expansion of this expression in terms of the actual atomic orbitals (for first row elements) and Slater-Condon factors is given in the Appendix.

The transition energies calculated in this manner then enter as the diagonal elements of the configuration interaction (CI) Hamiltonian. The off diagonal elements of the CI Hamiltonian are:

$$\begin{aligned}\langle{}^1\psi_0|H|{}^1\psi_{i\to a}\rangle &= 0 \qquad \text{(Brillouin's Theorem)}\\ \langle{}^1\psi_{i\to a}|H|{}^1\psi_{j\to b}\rangle &= 2(ai|jb)-(ab|ij)\,.\end{aligned} \qquad (11)$$

The triplet states are also calculated by this method by means of Eq. (7) from the value of the Coulomb integral, J_{ia}. However, the triplets will not be considered at present. The necessary scaling of the Coulomb integrals for the case of singlets partially corrects for electron correlation. Since triplet states might be expected to have very different electron correlation our choice of integrals for singlets may not be as appropriate.

c) Parameterization

Many models have been suggested for the evaluation of the Coulomb integrals. After an examination of several of these ideas, we chose a modification of the Mataga-Nishimoto recipe [10]

$$\gamma_{AB}=\frac{f_\gamma}{2f_\gamma/(\gamma_{AA}+\gamma_{BB})+R_{AB}} \qquad (12)$$

where R_{AB} is the distance between the two centers in Bohr radii. γ_{AA} is obtained from Pariser's observation [11]

$$\gamma_{AA}=F^0(AA)=I_A-A_A \qquad (13)$$

the values of which are presented in Table 1. The modification is the introduction of the parameter f_γ as suggested by Weiss [12], which we set equal to 1.2. This has the effect of raising the value of the two-center integral above that of the unmodified recipe. The value of 1.2 was chosen to reproduce the benzene spectrum, and especially the second excited singlet ($^1B_{1u}$), which is difficult to reproduce by any other recipe.

Table 1. Atomic parameters (eV)

	I_s	I_p	$G^1(sp)$	$F^2(pp)$	F^0	β
H	-13.06^a				12.85	-9.00
C	-19.84	-10.93	6.90	4.51	11.11	-17.00
N	-25.69	-14.05	8.96	6.46	12.01	-26.00

$f_\gamma = 1.2$ [Eq. (12)]: $f_\pi = 0.585, f_\sigma = 1.266$ [Eq. (15)].

[a] Calculated with $\zeta = 1.2$.

The two-center Fock elements are given by

$$F_{\mu\nu} = \bar{S}_{\mu\nu}(\beta_A + \beta_B)/2 - P_{\mu\nu}\gamma_{\mu\nu}/2\,. \tag{14}$$

In Eq. (14) β_A is a bonding parameter characteristic of atom A. $\bar{S}$ is a special overlap related to the ordinary orbital overlap S by

$$\begin{aligned} \bar{S}_{msns} &= S_{msns} \\ \bar{S}_{msnp} &= S_{msnp} \\ \bar{S}_{mpnp} &= f_\sigma G_\sigma S_{mp\sigma np\sigma} + f_\pi G_\pi S_{mp\pi np\pi} \end{aligned} \tag{15}$$

where G_σ and G_π are the appropriate geometric factors necessary to rotate the overlap from the local diatomic system to the molecular system, and f_σ and f_π are empirical factors adjusted to give the best agreement with experiment. Del Bene and Jaffé also found necessary a scaling down of the π–π two-center interaction: we have found a scaling up of the σ–σ interaction greatly beneficial. Both of these scalings can be justified from an examination of *ab-initio* calculations, properly core orthogonalized and symmetrically orthogonalized. This investigation, however, might suggest that these scaling factors, especially f_σ, be distance dependent.

From Eq. (14) it is apparent that the values of β, f_σ and f_π are coupled in their effect on the Fock matrix. We fit the product of $f_\pi\beta_C$ to reproduce the benzene spectrum, and then evaluate f_σ, β_C, f_π, β_N from the spectrum of pyridine. β_H is then obtained from its effect on the spectra of benzene, pyridine and pyrrole. The values we derive for β are given in Table 1, and are identical to those of Del Bene and Jaffé. The values of f_σ and f_π are also given in Table 1: the value of f_π is that of Del Bene and Jaffé.

Procedures

LCAOSCF-MO calculations using the INDO/1 approximation outlined in the previous section were done for benzene and several nitrogen-containing heterocycles-pyrrole, pyridine, pyrazine, pyrimidine, pyridazine, symmetric triazine, symmetric tetrazine, naphthalene, and quinoxaline (Fig. 1).

The computer programme used performs the INDO/1 calculation, with the parameterization outlined previously, from an input of molecular geometry and atomic numbers. A ground state calculation is followed by a configuration

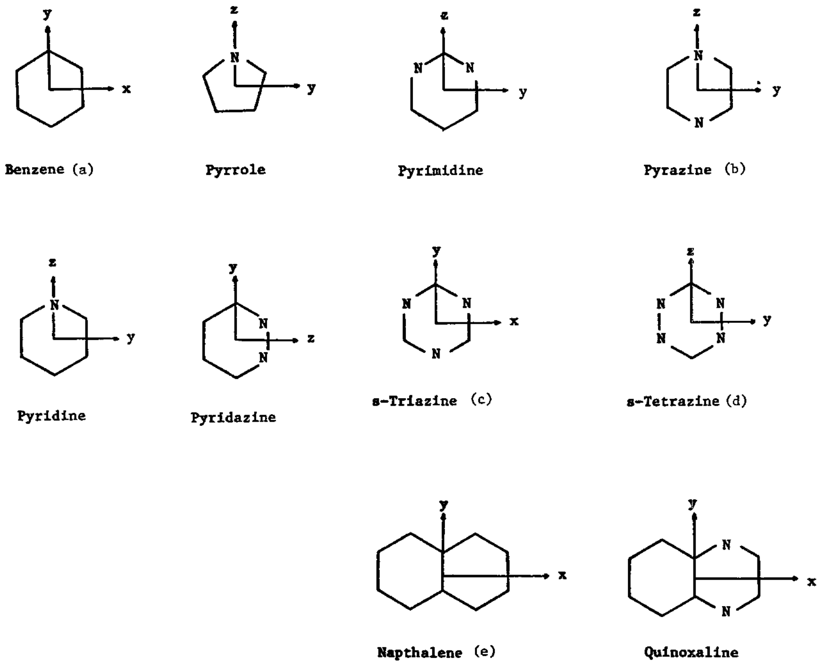

Benzene (a) Pyrrole Pyrimidine Pyrazine (b)

Pyridine Pyridazine s-Triazine (c) s-Tetrazine (d)

Napthalene (e) Quinoxaline

Fig. 1. Nitrogen containing heterocycles of this study, and the axis convention. References are for coordinates. a) Bacon, G. E., Curry, N. A., Wilson, S. A.: Proc. Roy. Soc. **279** A, 98 (1964). b) Wheatly, P. J.: Acta Cryst. **10**, 182 (1957). c) Wheatly, P. J.: Acta Cryst. **8**, 224 (1955). d) Bertinotti, F., Giacomello, G., Liquori, A. M.: Acta Cryst. **9**, 510 (1956). e) Cruickshank, D. W. J.: Acta Cryst. **10**, 504 (1957)

interaction calculation which results in the desired spectroscopic transition energies and oscillator strengths. These oscillator strengths are estimated using the dipole length operator. The dipole length evaluation includes the one center charge and polarization terms, but neglects two center "bond" contributions.

The molecular coordinates used in the calculation were obtained from the crystallographic data referenced in Fig. 1. When such data was not available, bond lengths and angles were estimated from those of representative compounds.

The parameters chosen for this study are based solely on the results obtained for benzene and pyridine. No attempt was made to optimize these parameters over the series of molecules studied. Consequently, some adjustment of parameters may result in a better over-all agreement with experiment. Occasionally we have shifted parameters in specific molecules where agreement was not especially good, and found our results insensitive to modest change.

Where the experimental information was definitive, we have calibrated calculated results to band maxima ($\nu_{\max}$). This seems most reasonable as we are estimating a point of the potential surface of the ground state near its experimental minimum, and points on the potential surface of excited states which are directly above the ground state minimum (Frank-Condon principale). What is observed is $\nu_{\max} = Te' + V_0' + V' - Te'' - V_0'' - V''$ where Te represents the global minimum of the potential energy curve, V_0 the zero point vibrational energy, V the vibrational energy above V_0, and the primes and double primes represent the excited state and the ground state respectively. Most often, $V''=0$. When the geometry of the ground and excited state is identical, we calculated $Te'-Te''=\nu_{\text{calc}}$ and $\nu_{\max}=\nu_{00}=\nu_{\text{calc}}+(V_0'-V_0'')$. The intrinsic error between calculation and experiment is caused by differences in the vibrational structure of the two states. If the excited state geometry is quite different, $\nu_{\text{calc}}=Te'+V_0'+V'-Te''$, and $\nu_{\max}=\nu_{\text{calc}}-V_0''$, where V_0'' for a large molecule is a sizeable quantity. The tacit assumption here, then, is that the excited states have similar geometries to the ground state, or at least their minima differ only along few normal coordinates. Our calculations then might be greater than the observed $\nu_{\max}$ by the zero point energy of the corresponding vibrations.

Choosing proper configurations for the excited state configuration interaction is an art, and in this it is difficult to claim we are artists. For pyrrole, benzene, and benzene analogues we have included all configurations that lie up to $\sim 75000\ \text{cm}^{-1}$ above the ground state, as well as some additional selected configurations (all π–π^* plus others of interesting symmetry type). Inclusion of excitations with energies much above this value seems unreasonable as we have not included double excitations, which generally start to appear at $\sim 85000\ \text{cm}^{-1}$; nor have we a mechanism for including Rydberg states which begin to occur in these molecules as low as $\sim 55000\ \text{cm}^{-1}$. The calculated energies of the first five to six excited states appear to be relatively stable to additional configuration interaction; states calculated to be higher than $\sim 60000\ \text{cm}^{-1}$ are still somewhat sensitive. We believe, however, that the limited CI performed (generally 45–55 singly excited configurations) is not a factor affecting our comparisons with experiment. Shortcomings in the correlation with experiment are attributed to shortcomings of the model itself.

In general, the Hartree-Fock scheme produces occupied orbitals appropriate for an n-electron system and virtual orbitals for an $(n+1)$-electron system [13]. Our parameterization on spectra might be expected to alter this, and reproduce a more balanced transition state. If we assume that our occupied orbitals are appropriate for an $(n-1/2)$-electron system, and our virtual orbitals for an $(n+1/2)$ system, then we reproduce a transition state, half way between the neutral species and positive (negative) ion, which is also useful in estimating ionization potentials (electron affinities) from orbital eigenvalues. Where possible, we have made this comparison.

Results

Throughout this section we will make heavy use of the compilation of experimental data on the azines by Innes, Byrne and Ross and their interpretation of this data.

a) Benzene

Benzene calculations were used to obtain values for the product of parameters $f_\pi \beta_C$, and to set a value of 1.2 for the factor "f_γ" in the Mataga-Nishimoto formula for the Coulomb repulsion integrals. These parameters were adjusted to give spectral results which are in good agreement with the experimentally determined $\nu_{\max}$ (Table 2).

The *uv* spectrum of benzene is well known to have three dominant π–π^* bands: $^1B_{2u} \leftarrow {}^1A_{1g}$, $^1B_{1u} \leftarrow {}^1A_{1g}$ and $^1E_{1u} \leftarrow {}^1A_{1g}$. The first two of these transitions are dipole forbidden, while the third is allowed with an experimental oscillator strength of 0.690. The results obtained for these three bands are very good; it is noted that the use of the Mataga-Nishimoto formula and the introduction of the INDO terms into the calculation have cause the $^1B_{1u}$ state to rise considerably in value over that calculated with the Pariser and Parr formula [11, 5]. Indeed this state is now calculated to be exactly where it is found by experiment.

It is reported by Parkin and Innes [14] that there is some intensity in the benzene spectrum over 60000 cm^{-1}. They believe that this may result from the presence of σ–π^* transitions. In these calculations, a series of π–σ^* states has been found in the region over 59000 cm^{-1}. Above this the density of electronic states is calculated to be high. None of these states, however, are calculated to have intensity.

The calculated oscillator strength for the $^1E_{1u}$ (π–π^*) transition is 2.1, roughly three times the observed value. This is a common observation: intense transitions are calculated two to four times more intense than observed. A rather large

Table 2. Benzene

Observed[a]				Calculated			
Symmetry	Type	Energy (cm^{-1})	Oscillator strength	Symmetry	Type	Energy (cm^{-1})	Oscillator strength
$^1B_{2u}$	π–π^*	38090	0.001	$^1B_{2u}$	π–π^*	37964	0.0
$^1B_{1u}$	π–π^*	48972	0.100	$^1B_{1u}$	π–π^*	48951	0.0
$^1E_{1u}$	π–π^*	55900[b]	0.690	$^1E_{1u}$	π–π^*	54957	2.14(x,y)
	(σ–π^*)	>60000		$^1E_{2u}$	π–σ^*	59459	0.0

[a] Ref. [14].

[b] $\nu_{\max}$ value. (Those bands not marked as $\nu_{\max}$ are 0–0 bands).

Table 3. Orbital energies of benzene (eV)

Ionization potentials[a]	Calculated		
	This work	*Ab-initio*[b]	
9.24	9.0	10.2	$1e_{1g}(\pi)$
11.5	12.6	14.3	$3e_{2g}$
12.3	13.4	14.6	$1a_{2u}(\pi)$
13.8	15.3	16.9	$3e_{1u}$
14.7	17.3	17.8	$1b_{2u}$
15.4	17.5	18.0	$2b_{1u}$
16.9	23.6	20.1	$3a_{1g}$
19.2	25.1	23.0	$2e_{2g}$
22.8	32.7	28.2	$2e_{1u}$

[a] Ref. [16]. – [b] Ref. [18].

body of evidence seems to suggest that employment of the velocity operator instead of the dipole length operator [15] does much to correct this deficiency, at least for larger molecules. The calculated oscillator strength within the CNDO approximation is 2.4: the reduction to 2.1 has been accomplished by a rather small admixing of σ–σ^* states ($\sim 3\%$ each state) through the additional INDO terms of the CI.

The first three π–π^* transitions in benzene set a pattern for the other compounds under investigation, for the other molecules may be viewed as perturbations of the benzene system. The success of the calculations for benzene gives some confidence that the chosen parameters will be suitable in the other cases examined.

Table 3 compares calculated molecular orbital energies with ionization potentials of benzene as determined using photo-electron spectroscopy [16]. As is often the case with *ab-initio* calculations, the first few ionization potentials agree fairly well, while the deeper ones are generally calculated too low. This trend may well be a shortcoming of Koopmann's approximation: relaxation processes becoming more important for the deeper electron holes. At any rate, a reparameterization of the entire CNDO technique seems necessary to obtain better agreement (see, for example, Ref. [17]).

The symmetry assignment of the photo-electron spectra is the same as that obtained from the *ab-initio* calculations of Schulman and Moskowitz [18], and that inferred from experimental substitution [16]. The bands at 12.3 eV and 14.7 eV appear as poorly resolved structures, overlapping other bands. It is interesting to note that if the band at 12.3 eV is associated as part of the e_{2g} structure (split through the Jahn-Teller effect), the calculated and observed results are in far better accord. Against this reinterpretation stands the fact that Fridh, Åsbrink, and Lindholm [17] were able to accurately reproduce all the experimental numbers with a modified INDO technique. The $1b_{2u}$ and $2b_{1u}$ states are calculated nearly degenerate in this work, and in the calculations reported here by Schulman and Moskowitz. The position of the $1b_{2u}$, however, appears to be very basis set dependent [18].

b) Pyridine

Pyridine was used to complete the parameterization by determining values for β_C^0, β_N^0 and f_σ. By varying these factors a good fit was obtained for the pyridine spectrum (Table 4).

The electronic spectrum of pyridine closely resembles that of benzene in that the presence of the nitrogen atom can be regarded as a perturbation which breaks the symmetry. In C_{2v} the "${}^1B_{2u}$" and "${}^1B_{1u}$" states of benzene are now allowed. The presence of the lone pair is responsible for two calculated n–π^*[1] transitions, one of which at 34771 cm^{-1} is symmetry allowed and is observed experimentally as sharp bands overlapping the ${}^1B_2({}^1B_{2u})$ π–π^* band at $\sim 38350\ \text{cm}^{-1}$. The second n–π^* transition is calculated to lie at $\sim 44000\ \text{cm}^{-1}$ and has not been observed. The next two π–π^* bands are observed as broad, allowed systems; the second of these, with $\nu_{\max} \sim 55000\ \text{cm}^{-1}$, is correlated with

---

[1] If the sum of the product of nitrogen coefficients squared times the square of the coefficient of the configuration in the state of interest is greater than 0.5, we will call the excitation $n\rightarrow$, if not, $\sigma\rightarrow$.

Table 4. Pyridine

Observed[a]				Calculated			
Symmetry	Type	Energy (cm^{-1})	Oscillator strength	Symmetry	Type	Energy (cm^{-1})	Oscillator strength
$^1B_1$	n–π^*	34771	~0.003	$^1B_1$	n–π^{*c}	34702	0.010(x)
$^1B_2$	π–π^*	~38350[b]	~0.04	$^1B_2$	π–π^*	38611	0.066(y)
				$^1A_2$	n–π^*	43984	0.0
$^1A_1$	π–π^*	49750	~0.10	$^1A_1$	π–π^*	49684	0.062(z)
$^1B_2$, $^1A_1$	π–π^*	~55000	~1.3	$^1A_1$	π–π^*	56861	0.909(z)
				$^1B_2$	π–π^*	56868	0.882(y)
$^1A_1$, $^1B_2$?	π–π^*	~56405	*diffuse*	$^1A_2$	π–σ^*	59363	0.0
				$^1B_1$	n–π^*	61803	0.01(x)
				$^1B_2$	π–π^*	62660	0.01(y)

[a] Ref. [19].

[b] diffuse, ν_{max} ~39000 cm^{-1}, see Ref. [20].

[c] All orbitals of σ symmetry with greater than 50% nitrogen character are designated as "n".

Table 5. Orbital energies of pyridine (eV)[a]

Ionization potentials	Calculated		
	This work	Clementi[b]	
9.28 (π)	9.14	12.16	$1a_2(\pi)$
10.54	10.02	12.49	$2b_1(\pi)$
12.22 (π)	10.16	12.65	$11a_1$
(13.43)	13.14	15.77	$7b_2$
14.44	14.20	16.93	$1b_1(\pi)$
15.49	14.40	17.40	$10a_1$
16.94	15.16	18.23	$6b_2$
(19.39)	17.43	19.07	$9a_1$
(20.14)	18.91	19.75	$5b_2$
	22.93	21.20	$8a_1$
	25.96	25.08	$7a_1$
	25.98	24.60	$4b_2$

[a] Parentheses around experimental values indicate uncertainties, see Ref. [21].

[b] Ref. [22].

the $^1E_{1u}$ in benzene. The calculated oscillator strength of 1.8 is in much better agreement with the observed value of 1.3 than in the corresponding case of benzene. The σ–σ^* admixing in this case is ~ 9% in both states.

Above 56000 cm^{-1} is observed a broad diffuse system overlapping with the preceding intense one. The calculations show many bands crowded above 59000 cm^{-1}, three of which are presented in Table 2. Several of these transitions are group theoretically allowed but are calculated to have little intensity.

The ionization potentials found for pyridine by Al-Jobourg and Turner are illustrated in Table 5, along with the calculated values. The agreement is satisfactory with the assignments of Al-Jobourg with the exception of the $2b_1(\pi)$ calculated at 10.02 eV and assigned at 12.22 eV, if the nearly degenerate $1b_1(\pi)$ and $10a_1(\sigma)$ are both assigned to the band observed at 14.44 eV.

For comparison, the eigenvalues obtained by Clementi [22] from an *ab-initio* Gaussian calculation are also presented in Table 5. With the exception of the $4b_2(\sigma)$ molecular orbital, our order is the same as Clementi's. Of interest is the fact that the *ab-initio* calculation also predicts the $11a_1(\sigma)$ and $2b_1(\pi)$ nearly degenerate.

Table 6. Pyrrole

Observed[a,b]				Calculated			
Symmetry	Type	Energy (eV)	Oscillator strength	Symmetry	Type	Energy (eV)	Oscillator[c] strength
	π–π^*	~5.7[e]	Very diffuse	$^1A_1$	π–π^*	5.51	0.004(z)
				$^1B_2$	π–π^*	5.51	0.269(y)
	π–π^*	6.5[e]	Continuum	$^1B_1$	π–σ^*	6.47	0.001(x)
				$^1A_2$	π–σ^*	6.57	0.0(f)
	π–π^*	7.1[e]	Weak, diffuse	$^1A_1$	π–π^*	7.13	0.824(z)
				$^1B_2$	π–π^*	7.36	0.217(y)
				$^1A_2$[d]	π–σ^*	7.80	0.0(f)
		8.2[e]	Single, sharp band	$^1B_1$[d]	π–σ^*	8.03	0.002(x)

[a] Ref. [24].

[b] Ref. [25].

[c] The letter in parentheses denotes the polarization; "f" is forbidden.

[d] Above 7 eV the configuration interaction is somewhat thin: the calculated value of this transition must be considered as suggestive only.

[e] $\nu_{\max}$ value

Table 7. Molecular orbital energies (eV)

Pyrrole[a]	Pyridazine	Pyrimidine	Pyrazine[b]	s-Tetrazine
8.01 $1a_2(\pi)$	9.40 $8b_2$	9.83 $2b_1(\pi)$	9.29 $1b_{1g}(\pi)$	10.27 $3b_{3g}$
9.29 $2b_1(\pi)$	9.68 $1a_2(\pi)$	9.94 $8b_2$	9.95 $6a_g$	10.84 $1b_{2g}(\pi)$
13.75 $6b_2$	10.50 $2b_1(\pi)$	10.82 $1a_2(\pi)$	11.25 $1b_{2g}(\pi)$	12.00 $5b_{1u}$
13.92 $9a_1$	11.64 $11a_1$	11.23 $11a_1$	11.62 $5b_{1u}$	12.34 $1b_{1g}(\pi)$
14.67 $1b_1(\pi)$	14.40 $10a_1$	14.51 $10a_1$	14.08 $3b_{3g}$	12.83 $6a_g$
15.47 $8a_1$	14.52 $7b_2$	14.66 $7b_2$	15.00 $1b_{3u}(\pi)$	12.96 $4b_{2u}$
15.86 $5b_2$	15.18 $1b_1(\pi)$	15.10 $1b_1(\pi)$	15.04 $4b_{2u}$	16.24 $1b_{3u}(\pi)$
22.56 $7a_1$	17.76 $6b_2$	16.63 $9a_1$	18.00 $4b_{1u}$	17.13 $4b_{1u}$
23.18 $4b_2$	20.44 $9a_1$	20.25 $6b_2$	20.36 $3b_{2u}$	21.01 $5a_g$
24.32 $6a_1$	23.14 $8a_1$	22.79 $8a_1$	21.80 $5a_g$	23.37 $3b_{2u}$

[a] *Ab-initio* calculations by Clementi [22] indicate several order reversals.

[b] The order is the same as that obtained by Clementi [22] with the single reversal of $1b_{1g}(\pi)$ and $6a_g$ (see text).

c) Pyrrole

Three of the five *pi* molecular orbitals of pyrrole are filled. A simple analysis would lead one to expect three π–π^* transitions in the near *uv*-visible region. Bands centered at 5.57, 6.5 and 7.1 eV have been assigned as π–π^*, but such an assignment has been difficult to ascertain both experimentally [23] and theoretically [2]. The present calculations indicate a more interesting assignment, as shown in Table 6. The numerical precession lends some degree of confidence to the assignments. Two transitions are calculated at 6.5 eV, both of which are π–σ^* type. Reasonable reparameterization will not greatly split the degeneracy of the two π–π^* bands reported at 5.5 eV.

The orbital energies found for pyrrole are given in Table 7. The observed value for the first ionization potential is 8.9 eV [24].

d) Pyridazine (1,2-diazine)

The principal features of the π–π^* spectra of the diazines can again be considered to be derived from a perturbation of benzene. Three π–π^* bands are observed; the presence of lone pairs introduces additional structure.

The lowest band of pyridazine, of $^1B_1$ symmetry, is calculated at 25150 cm^{-1} in good accord with the experimental band at 26649 cm^{-1} [19], Table 8. There seems to be little evidence for the $^1A_2\,(n-\pi^*)$ band calculated at 33500 cm^{-1}, nor that calculated at 45600 cm^{-1}. Both are formally forbidden. The $^1B_2\,(\pi$–$\pi^*)$ and $^1B_1\,(n$–$\pi^*)$ found nearly degenerate at ~51000 cm^{-1}, are calculated nearly degenerate at ~50000 cm^{-1}. The experimental assignments appear somewhat

Table 8. Pyridazine

Observed[a]				Calculated			
Symmetry	Type	Energy (cm^{-1})	Oscillator strength	Symmetry	Type	Energy (cm^{-1})	Oscillator strength
$^1B_1$	n–π^*	26649	~0.0058	$^1B_1$	n–π^*	25155	0.016(x)
				$^1A_2$	n–π^*	33482	0.0
$^1A_1$	π–π^*	39500	~0.020	$^1A_1$	π–π^*	40543	0.058(y)
				$^1A_2$	n–π^*	45642	0.0
$^1B_2$	π–π^*	~50000	~0.10 (continuous)	$^1B_2$	π–π^*	50440	0.069(z)
$^1B_1$?	n–π^*	50865 or 51503		$^1B_1$	$n-\pi^*$	49760	0.011(x)
				$^1B_1$	n–π^*	57317	0.004(x)
$^1B_2$, $^1A_1$?	π–π^*	57300		$^1B_2$	π–π^*	57486	0.851(z)
				$^1A_1$	π–π^*	57964	0.783(y)
	(R)	Not observed					

[a] Ref. [19].

uncertain [14, 19]. Unfortunately, one cannot distinguish the order of bands calculated so near in energy with much confidence.

The orbital energies of pyridazine are reported in Table 7. The first ionization potential is observed at 8.91 eV [26].

e) Pyrimidine (1,3-diazine)

The electronic spectrum of pyrimidine is illustrated in Table 9. Three π–π^* bands are found. The π–π^* band ($^1A_1$, $^1B_1$?) lying highest in energy is described

Table 9. Pyrimidine

Observed[a]				Calculated			
Symmetry	Type	Energy (cm^{-1})	Oscillator strength	Symmetry	Type	Energy (cm^{-1})	Oscillator strength
$^1B_1$	n–π^*	31073	~0.0069	$^1B_1$	n–π^*	32392	0.015(x)
$^1A_2$?	n–π^*	?		$^1A_2$	n–π^*	36286	0.0
$^1B_2$	π–π^*	40310	~0.052	$^1B_2$	π–π^*	41648	0.076(y)
				$^1A_2$	n–π^*	43236	0.0
$^1B_1$?	n–π^*	51143?	~0.005	$^1B_1$	n–π^*	49979	0.009(x)
$^1A_1$?	π–π^*	52340?	~0.16	$^1A_1$	π–π^*	52819	0.084(z)
$^1A_1$	R	56271	~0.25				
$^1A_1$, $^1B_1$?	π–π^*	~58500	~1	$^1A_1$	π–π^*	59304	0.795(z)
				$^1A_2$	n–π^*	60143	0.0
				$^1B_2$	π–π^*	60808	0.817(y)

[a] Ref. [19].

Table 10. Pyrazine

Observed[a]				Calculated			
Symmetry	Type	Energy (cm^{-1})	Oscillator strength	Symmetry	Type	Energy (cm^{-1})	Oscillator strength
$^1B_{2g}$?	n–π^*	~30425?					
$^1B_{3u}$	n–π^*	30875	~0.010	$^1B_{3u}$	n–π^*	28513	0.014(x)
$^1B_{2u}$	π–π^*	37839–38808	~0.10	$^1B_{2u}$	π–π^*	37361	0.179(y)
				$^1B_{2g}$	n–π^*	37768	0.0
				^1A_u	n–π^*	40993	0.0
$^1B_{1u}$	π–π^*	50880	~0.15	$^1B_{1u}$	π–π^*	50068	0.196(z)
$^1B_{3u}$?	n–π^*	54000?	Fragmentary	$^1B_{1g}$	n–π^*	55790	0.0
$^1B_{2u}$	R	55154					
$^1B_{2u}$, $^1B_{1u}$	π–π^*	60700	~1.0	$^1B_{1u}$	π–π^*	60016	0.578(z)
				$^1B_{2g}$	n–π^*	61043	0.0
				$^1B_{3g}$	π–π^*	61833	0.0
				$^1A_{1u}$	π–σ^*	62734	0.0
				$^1B_{2u}$	π–π^*	62764	0.799(y)
$^1B_{2u}$	R	65746					

[a] Ref. [19].

as being very diffuse – its identity as a separate system is based on an analogy with pyrazine. The calculations show two π–π^* bands (the ${}^1E_{1u}$ of benzene) separated by about 1500 cm^{-1}, both with high intensity, in this region.

The lower lying π–π^* transitions are calculated very nearly where they are observed. The assignment of the ${}^1A_1$ (π–π^*) band at 52340 cm^{-1} is verified. As with pyridazine, two ${}^1A_2$ (n–π^*) bands are calculated at approximately 35000 cm^{-1} and 45000 cm^{-1}. In this case, however, there appears to be some evidence for the existence of the lower of the two [27].

The first ionization potential of pyrimidine is observed at 9.83 eV [26]. The orbital energies calculated are listed in Table 7.

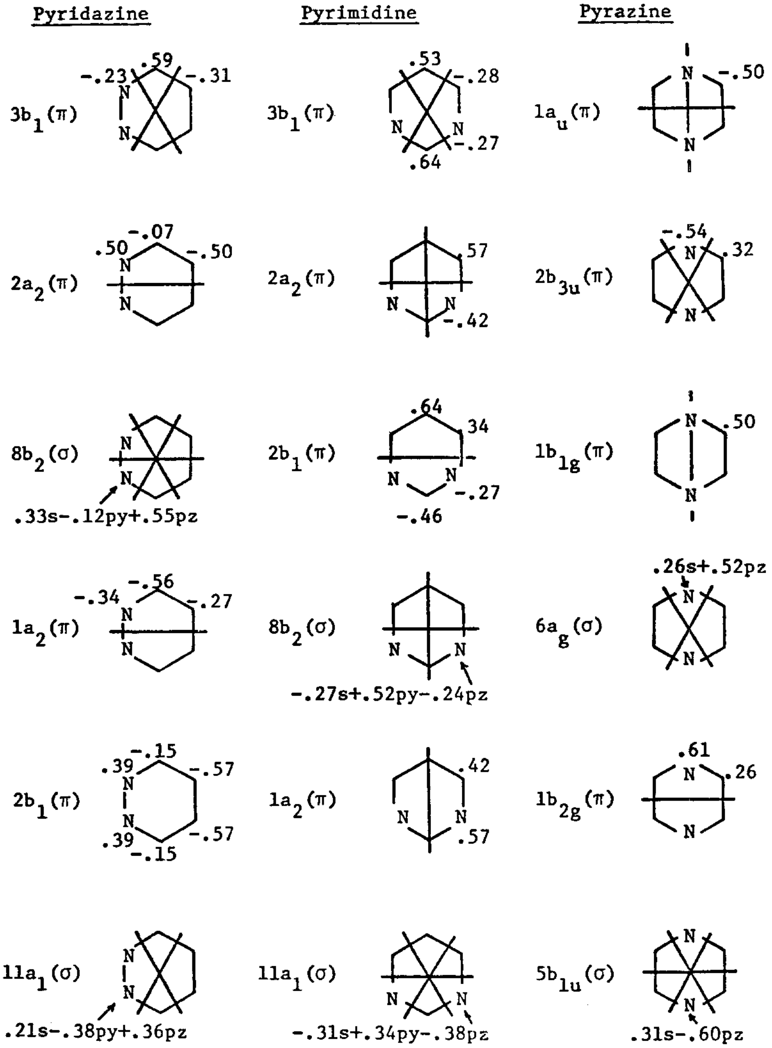

Fig. 2. Nodal patterns of the diazines. The diagrams are arranged in increasing energy order; the bottom three are doubly occupied. Numbers refer to M.O. coefficients

f) Pyrazine (1,4-diazine)

Three π–π^* bands are observed to be centered at $\sim 38300\,\text{cm}^{-1}$ ($^1B_{2u}$), $\sim 50900\,\text{cm}^{-1}$ ($^1B_{1u}$) and $61000\,\text{cm}^{-1}$ ($^1B_{1u}$, $^1B_{2u}$), in good agreement with the calculated values $37400\,\text{cm}^{-1}$, $50100\,\text{cm}^{-1}$, and two bands at $60000\,\text{cm}^{-1}$ ($^1B_{1u}$) and $62800\,\text{cm}^{-1}$ ($^1B_{2u}$), Table 5. The latter two bands (the split $^1E_{1u}$ of benzene) are calculated to enclose three other transitions. One of these is $^1B_{2g}$ (π–π^*) which might do considerable damage to the band. This system, which is higher in energy than the corresponding $^1E_{1u}$ bands of benzene, is reported to be very diffuse with a weakly developed structure.

The lowest transition is calculated as $^1B_{3u}$ (n–π^*). We find no low lying $^1B_{2g}$ (n–π^*) and thus question the assignment given the band found in pure crystals at $\sim 30400\,\text{cm}^{-1}$ [27]. In all the diazines we find the lowest singlet transition to be of the same nature: from a sigma orbital with between 67% (pyrazine) and 82% (pyridazine, pyrimidine) assymmetric nitrogen lone pair to the two-noded π^* counterpart of the e_{2u} molecular orbital of benzene with the most amount of nitrogen character.

The observed band at $54000\,\text{cm}^{-1}$ is assigned $^1B_{1g}$ (n–π^*), and its counterpart is found in all three diazines. At first glance the assignment would seem odd as B_1 (in C_{2v} for pyrimidine and pyridazine) corresponds to B_{3u} (in D_{2h} for pyrazine) and not to B_{1g} (as assigned in the calculation). The principal π molecular orbital involved is this transition is the two-noded component of the benzene e_{2u} with the least nitrogen character: for pyrazine this molecular orbital has a node through the nitrogens, for pyridazine and pyrimidine it has nodes through the bonds, Fig. 2. The σ molecular orbital leading to the transition is between 65% (pyrimidine and pyridazine) and 92% (pyrazine) the symmetric sum of nitrogen lone pairs.

The energies of the highest occupied molecular orbitals appear in Table 7. An ionization potential of 9.29 eV has been extrapolated from $^1B_{2u}$ ($2\pi \rightarrow n\pi$) Rydberg series [14]. A second value observed at 10 eV is attributed to the loss of a sigma electron [14]. Our calculation is in good accord, whereas the calculation of Clementi implies a reverse order [22].

g) s-Triazine

Extensive experimental data is not available for the higher excited states of symmetric triazine, Table 11. The $^1A_2'$ (π–π^*) transition reported at $44000\,\text{cm}^{-1}$ is in reasonable agreement with the calculated value of $45919\,\text{cm}^{-1}$. The first two n–π^* transitions reported [19, 28] have been recently reassigned by Fischer and Small [29]. The new assignment agrees with our calculated order; the $^1E''$ (n–π^*) is observed and calculated $\sim 1000\,\text{cm}^{-1}$ below the $^1A_2''$ (n–π^*). Both bands are calculated $\sim 4000\,\text{cm}^{-1}$ above their observed ν_{00} values. Modest changes in molecular geometry and parameterization do not appear to lessen this discrepancy to any great extent. As these transitions represent our worst agreement with experimental numbers, we cannot exclude the possibility of ignored configurations that would depress the calculated transition energies.

Table 11. *s*-triazine

Observed[a]				Calculated			
Symmetry	Type	Energy (cm^{-1})	Oscillator strength	Symmetry	Type	Energy (cm^{-1})	Oscillator strength
$^1A_2''^{b}$	n–π^*	31 574	~0.018	$^1E''$	n–π^*	35 817	0
$^1A_1''$, $^1E''^{b}$	n–π^*	32 500	Diffuse	$^1A_2''$	n–π^*	36 778	0.040(z)
				$^1A_1'$	n–π^*	38 474	0
$^1A_2'$	π–π^*	44 000	~0.002	$^1A_2'$	π–π^*	45 919	0
$^1A_2''$ or E'	R	55 782		$^1E''$	n–π^*	55 163	0
				$^1A_1'$	π–π^*	56 758	0
				$^1E'$	π–π^*	61 253	0.836(x,y)

[a] Ref. [19].

[b] Ref. [29] reverses these two assignments.

Table 12. Orbital energies for *s*-triazine (eV)

Ionization potentials[a]	Calculated
10.4(σ)	10.4 $6e'$
11.7[b](π) 12.2[b]	11.1 $1e''(\pi)$
13.2(σ)	13.5 $5a'$
14.6(π)	14.8 $5e'$
14.8	15.8 $1a_1''(\pi)$
17.9	21.6 $1a_2'$
22.3	23.6 $4a_1'$
	27.9 $4e'$

[a] Ref. [16].

[b] The splitting is attributed to Jahn-Teller effects (see text).

A more extensive CI calculation has eliminated the possibility of singly excited configurations contributing to a significant lowering.

A series of ionization potentials for *s*-triazine is illustrated in Table 12 along with the molecular orbital eigenvalues. As seen in the case of benzene, the first few calculated energies are in very good agreement with the experimental values, while the deeper values are calculated too low. Robin, Kuebler and Brundle [16] suggest that the observed values of 11.7 eV and 12.2 eV are associated with e'' (π) split by Jahn-Teller effects. This is consistent with our calculation as we find no band between $1e''$ (π) and $5a_1'$ (σ), but it does seem odd that no similar effect has been recognized in benzene. The experimental spectrum shows a broad structured band from ~ 14.5–16.0 eV with considerable assymetry on the high energy side. The $5e''$ (σ) and $1a_1''$ (π) are calculated to lie in this region. If the observed bands at 14.65 eV and 14.85 eV are assigned to $5e'$ (σ), the assymetry of the band could be prescribed to the $1a_1''$ (π). Such an interpretation would lead to the conclusion that there is little shift between this π molecular orbital and the corresponding one in cyanuric fluoride (tri-fluoro s-triazine), while the $1e''$ (π) shows a shift of 0.4 eV. This trend – that the $e(\pi)$ shift more than the $a(\pi)$ upon fluorination – is already noted for benzene and hexafluorobenzene [16].

h) s-Tetrazine

The observed spectrum of *s*-tetrazine is given in Table 13 where it is compared with the results of calculation. A $^1B_{3u}$ (n–π^*) transition is found at 18129 cm^{-1}; the calculation also predicts that the lowest transition is $^1B_{3u}$ (n–π^*) at 20500 cm^{-1}. A transition occurs at $\sim$31250 cm^{-1} and is seen as a shoulder on the next band. The calculations indicate a forbidden band at 31979 cm^{-1} of $^1B_{1g}$ symmetry. This n–π^* transition demonstrates an unusually high degree of configurational mixing; the $n_b \rightarrow \pi_{ab}$ pushed down by $n_{ab} \rightarrow \pi_{bbb}$ (n_{ab}-nodes through opposite atoms, opposite bonds, etc.). The π–π^* band has an onset at $\sim$35000 cm^{-1} with $\nu_{\max}$ at 40486 cm^{-1}, in good agreement with the calculation. At the onset ($\sim$35000 cm^{-1}) we note a calculated ^1A_u (n–π^*).

The calculated orbital energies for *s*-tetrazine are given in Table 7. We have not been able to find experimental values for comparison.

Table 13. *s*-tetrazine

Observed[a]				Calculated			
Symmetry	Type	Energy (cm^{-1})	Oscillator strength	Symmetry	Type	Energy (cm^{-1})	Oscillator strength
$^1B_{3u}$	n–π^*	18129	$\sim$0.0042	$^1B_{3u}$	n–π^*	20499	0.023(x)
$^1B_{3u}$?	n–π^*	$\sim$31250[b]	$\sim$0.001	$^1B_{1g}$	n–π^*	31979	0.0
		$\sim$35000?		^1A_u	n–π^*	34536	0.0
$^1B_{2u}$	π–π^*	40486[c]	Broad, structureless	$^1B_{2u}$	π–π^*	39262	0.190(y)
				$^1B_{2g}$	n–π^*	40160	0.0
				^1A_u	n–π^*	43387	0.0
				$^1B_{3u}$	n–π^*	51378	0.0
				$^1B_{1g}$	n–π^*	52689	0.0
				$^1B_{1u}$	π–π^*	53911	0.062(z)
				$^1B_{3u}$	n–π^*	57219	0.025(x)
				$^1B_{1u}$	π–π^*	59757	0.828(z)
				$^1B_{1g}$	n–π^*	62012	0.0
				$^1B_{2u}$	π–π^*	63713	0.554(y)

[a] Ref. [19]. – [b] band shoulder. – [c] $\nu_{\max}$ value.

i) Naphthalene

Preliminary calculations were made on naphthalene and quinoxaline in order to determine the validity of the method on larger systems. The results obtained for naphthalene are shown in Table 14 along with the experimental values reported by George and Morris [30].

Table 14. Naphthalene

Observed[a]				Calculated			
Symmetry	Type	Energy (cm^{-1})	Oscillator strength	Symmetry	Type	Energy (cm^{-1})	Oscillator strength
$^1B_{2u}$	π–π^*	32020	0.002	$^1B_{2u}$	π–π^*	32505	0.002(x)
$^1B_{1u}$	π–π^*	37500[b]	0.102	$^1B_{1u}$	π–π^*	37743	0.148(y)
				^1A_g	π–π^*	44759	0.0
$^1B_{2u}$	$\pi-\pi^*$	47530	1.0	$^1B_{2u}$	π–π^*	45823	1.866(x)
				$^1B_{3g}$	π–π^*	46707	0.0
$^1B_{1u}$	π–π^*	49510	0.3	$^1B_{1u}$	π–π^*	48630	0.672(y)
$^1B_{2u}$	π–π^*	52650	0.1	$^1B_{1g}$	π–σ^*	52672	0.0
				$^1B_{3g}$	π–π^*	52680	0.0
	R	>54000					
				^1A_g	π–π^*	55966	0.0
				$^1B_{2g}$	σ–π^*	57190	0.0
				$^1B_{2g}$	π–σ^*	57363	0.0
				⋮			
				$^1B_{2u}$	π–π^*	60510	0.115(x)

[a] Ref. [30]. — [b] ν_{max} value.

Five π–π^* transitions are observed in the vapour spectrum: the calculated values are in excellent agreement. The calculated oscillator strengths for these bands are also close to those observed. The calculations indicate forbidden π–π^* bands at 44759 cm^{-1} (^1A_g) and 46707 cm^{-1} ($^1B_{3g}$). A large number of forbidden bands are calculated to be in the region between 58000 cm^{-1} and 62000 cm^{-1}.

George and Morris report a band at 52650 cm^{-1}. On the basis of calculations by Hummel and Ruedenberg [31], and on the basis of the intensity of the band, it is assigned as $^1B_{2u}$. In this region we calculate two forbidden bands, $^1B_{1g}$ (π–σ^*) and $^1B_{3g}$ (π–π^*). The next band of $^1B_{2u}$ (π–π^*) we find at 60500 cm^{-1}, to be compared with Pariser's [32] estimate at 64700 cm^{-1}. Extensive singly excited configuration interaction of $^1B_{2u}$ states does not lower our calculated value significantly. The most likely explanation we have for the band observed at 52650 cm^{-1} is that it is $^1B_{3g}$, borrowing from the $^1B_{1u}$ band at 48630 cm^{-1} through one of the b_{2u} modes.

Analysis of the Rydberg bands beginning at 54000 cm^{-1} has led to an ionization potential of approximately 8.1 eV [33]. The calculated value of this orbital energy is 7.95 eV.

j) Quinoxaline

The observed spectrum of quinoxaline, Table 15, contains a $^1B_1$ (n–π^*) transition at 27071 cm^{-1} which is in good agreement with our calculated value of 26382 cm^{-1}. The first $^1A_1$ (π–π^*) band is observed and calculated at $\sim$ 31950 cm^{-1} (ν_{max} value). This system is reported to consist of broad structureless

Table 15. Quinoxaline

Observed[a]				Calculated			
Symmetry	Type	Energy (cm^{-1})	Oscillator strength	Symmetry	Type	Energy (cm^{-1})	Oscillator strength
$^1B_1$	n–π^*	27071		$^1B_1$	n–π^*	26382	0.013(z)
$^1A_1$	π–π^*	31959[b]		$^1A_1$	π–π^*	31916	0.156(x)
				$^1B_2$	π–π^*	34412	0.105(y)
				$^1A_2$	n–π^*	36248	0.0
				$^1A_2$	n–π^*	42309	0.0
$^1B_2$	π–π^*	43898[b]		$^1A_1$	π–π^*	42667	0.565(x)
		$\sim$48309		$^1B_2$	π–π^*	47179	0.092(y)
		$> \sim$50000		$^1A_1$	π–π^*	49509	1.017(x)
				$^1B_2$	π–π^*	50241	0.549(y)
				$^1B_1$	n–π^*	50954	0.0(z)

[a] Ref. [34]. — [b] $\nu_{\max}$ values.

bands [34], the structure of which is believed to be a manifestation of internal conversion mechanisms within the molecule [35]. We calculate a $^1B_2$ (π–π^*) of nearly equal intensity 2500 cm^{-1} from the $^1A_1$ (π–π^*), or within the reported structure for this band.

The second observed π–π^* band is seen at 43898 cm^{-1} to be broad and diffuse with intensity five times greater than that of the first π–π^*; our calculations are in good accord. There is evidence in the spectrum of a further band at $\sim$48300 cm^{-1} with intensity of approximately one fifth that of the previous band. The calculation produces a $^1B_2$ (π–π^*) at 47179 cm^{-1}.

We calculate two intense transitions at $\sim$50000 cm^{-1}; the observed spectrum shows great intensity in this region with onset $\sim$49000 cm^{-1}.

Many bands are calculated above $\sim$55000 cm^{-1}. Of particular interest are two allowed $^1B_2$ (π–π^*) states calculated at $\sim$58000 cm^{-1}.

The first few ionization potentials of quinoxaline are calculated as $a_2(\pi)$ 8.6 eV, $b_2(\pi)$ 8.8 eV, $a_1(60\%\ N_\sigma)$ 9.8 eV, $b_1(90\%\ N_\sigma)$ 11.5 eV, $a_2(\pi)$ 11.7 eV.

Discussions

a) Comparison With CNDO *Calculations*

The calculations reported here are in considerably better agreement with experiment than are the original calculations of Del Bene and Jaffé [5] that utilized the Pariser and Parr recipé [11] for the two electron Coulomb integrals. In a very recent paper, however, Ellis, Kuehnlenz and Jaffé [36] refined the original CNDO model of Del Bene and Jaffé, and incorporated the Mataga-Nishimoto formula for these integrals. A comparison of the results reported by Ellis *et al.* with those reported here might be expected to reflect principally the refinement

Table 16. Comparison of some CNDO and INDO calculations: eV (osc. strength)

		CNDO/*S*[a]	INDO/*S*[b]	*Obs*[c]
Pyridine	$^1B_1$	4.2(0.00)	4.3(0.01)	4.3(∼0.003)
	$^1B_2$	4.9(0.06)	4.8(0.07)	4.8(0.04)
	$^1A_2$	5.6(0)	5.5(0)	Not obs.
	$^1A_1$	6.0(0.22)	6.2(0.06)	6.2(0.1)
	$^1A_1$, $^1B_2$	6.8(0.76)	7.0(1.79)	7.0(∼1.3)
Pyrazine	$^1B_{3u}$	3.2(0.01)	3.5(0.01)	3.8(0.01)
	$^1B_{2u}$	4.8(0.16)	4.6(0.18)	4.8(0.10)
	$^1B_{2g}$	4.5(0)	4.7(0)	3.7?
	^1A_u	5.2(0)	5.1(0)	Not obs.
	$^1B_{1u}$	6.3(0.12)	6.3(0.20)	6.3(0.15)
	$^1B_{1g}$		6.9(0)	6.7–6.9
	$^1B_{1u}$	7.2(0.48)	7.4(0.58)	7.5(∼1.0)
	$^1B_{2g}$		7.6(0)	
	$^1B_{3g}$		7.7(0)	
	$^1A_{1u}$	7.2(0)	7.8(0)	
	$^1B_{2u}$	7.5(0.97)	7.8(0.80)	

[a] Ellis, Kuehnlenz, and Jaffé: Ref. [36].
[b] This work. – [c] Ref. [19].

in going from the CNDO to INDO approximations, although, to be sure, difference in the degree to which parameters have been optimized within the two models are a factor. Table 16 presents such a comparison of results for pyridine and pyrazine.

The results and conclusions reached for pyridine from both calculations are very similar. The numerical accuracy of the INDO technique developed within this paper seems better, but only marginally so if one considers that pyridine was one of the molecules on which we parameterized, and that the experimental values might be in doubt by as much as ± 0.1 eV.

The example of pyrazine is more typical of the comparison between results obtained by the two methods. Again the numerical accuracy is somewhat better for the INDO calculations. More important, however, is that some different conclusions are reached. The $^1B_{2g}$ state at 4.5 eV, calculated to lie below the allowed $^1B_{2u}$ (see Table 16) by the CNDO technique, has been assigned by Ellis *et al.* to the 3.7 eV band observed in pure crystals [27]. We calculate the $^1B_{2g}$ state to lie slightly above the allowed transition, and find it difficult to support the observation at 3.7 eV (see discussion on pyrazine). Extended CI within our model does not change these conclusions. The *ab-initio* studies of Hackmeyer and Whitten [37] confirm the order we obtain for these two states, but do indicate that the ^1A_u (n–π^*) might be the second excited singlet state, lying nearly degenerate with the $^1B_{2u}$. The observed band at 6.9 eV we assign to $^1B_{1g}$. The CNDO calculations have reported no counterpart for this state.

A more exhaustive comparison of results does not seem appropriate here, but rather might be of interest in trying to explain the observed spectrum of a specific molecule. In general the results obtained by the two techniques are similar: even so, assignments made by Jaffé and coworkers [5, 36] for observed bands are not always in agreement with those we have made.

b) Comments on the Model

We have refined a model for the calculation of electronic spectra which seems to be capable of good reliability, reasonable accuracy, and rapid execution. (The spectrum of symmetric triazine with 58 configurations is estimated on an IBM 370/155 in one minute). We have made no systematic attempt to optimize parameters, and it is possible that such an investigation might improve our "average" results. For the most part, however, the results appear to be relatively insensitive to all parameters except f_γ.

In a similar fashion the parameters f_γ, f_π and f_σ might be distance dependent, and we have assumed them constant. At large enough R, f_γ must equal unity, as $\gamma_{AB} \to f_\gamma / R_{AB}$. For $f_\gamma = 1.2$ [Eq. (4)] this aesthetically unpleasant conclusion is not reached until $R \sim 6$–8 Å, and the integral is already relatively small. f_π and f_σ [Eq. (7)] should probably approach unity also with increasing internuclear separation, but again, the overlap itself becomes small. f_σ, however, might be strongly distance dependent, especially in normal bonding situations. The $p_\sigma - p_\sigma$ overlap goes through a zero and then increases, before it uniformly decreases with increasing R. An examination of the integrals absorbed in $\beta\overline{S}$ reveals that they have this general behaviour also (see, for example, Ref. [7]), but their zero and maximum values do not coincide with those of the overlap. Such considerations indicate that f_σ should increase in value until the overlap maxima, which for $2p_\sigma$–$2p_\sigma$ interactions is the point when $\varrho = \bar{\zeta} R = 4.5$, where $\bar{\zeta}$ = average exponent. For much smaller values of ϱ Eq. (14) might become totally inappropriate. For non-nearest neighbor atoms $\varrho > 4.5$: the principle of maximum overlap gives for bonded atoms $\varrho \sim 4.5$. At any rate, our preliminary investigations on other molecules of quite different size and shape do not demonstrate any great deterioration of results.

Possible refinements to, and shortcomings of, the model not withstanding, we find that the results obtained are of sufficient accuracy to aid in the understanding of the singlet spectra of the compounds studied. It should be relatively straightforward to incorporate other atoms of interest into the scheme.

Since our parameters do not differ greatly from those chosen by Jaffé and Del Bene [5], their values should make appropriate starting choices when examining atoms not included in this study.

Acknowledgements. This work was supported in part by a research grant from the National Research Council of Canada. The basic configuration interaction program was written by one of us (M.Z.) in conjunction with Charles Warren while we were at the University of Uppsala, Sweden. His assistance is gratefully acknowledged, as is the hospitality and aid of Professor Löwdin and his Quantum Chemistry Group. Helpful discussions with Karl Weiss are cheerfully acknowledged.

Appendix

Added to the CNDO molecular integrals to convert the CI to INDO is the following correction.

$$\begin{aligned}
\text{Correction} = {} & \Sigma C_{i\alpha} C_{j\beta} C_{k\gamma} C_{l\delta} (\alpha\beta|\gamma\delta) \\
& [\alpha, \beta, \gamma, \delta] \in A \\
& \alpha \neq \beta \\
& \gamma \neq \delta \\
= {} & \{[C_{ix}C_{js} + C_{is}C_{jx}][C_{kx}C_{ls} + C_{ks}C_{lx}] \\
& + [C_{iy}C_{js} + C_{is}C_{jy}][C_{ky}C_{ls} + C_{ks}C_{ly}] \\
& + [C_{iz}C_{js} + C_{is}C_{jz}][C_{kz}C_{ls} + C_{ks}C_{lz}]\} \frac{G^1}{3} \\
& + \{[C_{ix}C_{jy} + C_{iy}C_{jx}][C_{kx}C_{ly} + C_{ky}C_{lx}] \\
& + [C_{ix}C_{jz} + C_{iz}C_{jx}][C_{kx}C_{lz} + C_{kz}C_{lx}] \\
& + [C_{iy}C_{jz} + C_{iz}C_{jy}][C_{ky}C_{lz} + C_{kz}C_{ly}]\} \frac{3}{25} F^2 \\
& + \{C_{ix}C_{jx}C_{kx}C_{lx} + C_{iy}C_{jy}C_{ky}C_{ly} + C_{iz}C_{jz}C_{kz}C_{lz}\} \frac{4}{25} F^2 \\
& - \{[C_{ix}C_{jx}C_{ky}C_{ly} + C_{iy}C_{jy}C_{kx}C_{lx}] \\
& + [C_{ix}C_{jx}C_{kz}C_{lz} + C_{iz}C_{jz}C_{kx}C_{lx}] \\
& + [C_{iy}C_{jy}C_{kz}C_{lz} + C_{iz}C_{jz}C_{ky}C_{ly}]\} \frac{2}{25} F^2
\end{aligned}$$

References

1. Parr, R. G.: The quantum theory of molecular electronic structure. W. A. Benjamin, Inc. 1964
2. Fischer-Hjalmers, I.: Acta Chem. Scand. **22**, 607 (1968)

3a. Pople, J. A., Santry, D. P., Segal, G. A.: J. Chem. Phys. **43**, S 129 (1965)

3b. Pople, J. A., Segal, G. A.: J. Chem. Phys. **43**, S 136 (1965)

3c. Pople, J. A., Segal, G. A.: J. Chem. Phys. **44**, 3289 (1966)

4. Pople, J. A., Beveridge, D. L., Dobosh, P. A.: J. Chem. Phys. **47**, 2026 (1967)
5. Del Bene, J., Jaffé, H. H.: J. Chem. Phys. **48**, 1807 (1968); **48**, 4050 (1968)
6. Slater, J. C.: Phys. Rev. **36**, 57 (1930)
7. Zerner, M. C.: In: Herman, F., McLean, A. S., Nesbet, R. K. (Eds.): Computational methods for large molecules, p. 117, New York, London: Plenum Press, 1973
8. Moore, C. E.: Atomic energy levels. U.S. Department of Commerce, National Bureau of Standards, Circular 467 (1949)
9. Hinze, J., Jaffé, H. H.: J. Chem. Phys. **38**, 1834 (1963)
10. Mataga, N., Nishimoto, K.: Z. Physik. Chem. (Frankfurt) **13**, 140 (1957)
11. Pariser, R., Parr, R. G.: J. Chem. Phys. **21**, 767 (1953)
12. Weiss, K.: Private communication (1970)
13. Roothaan, C. C. J.: Rev. Mod. Phys. **23**, 69 (1951)
14. Parkin, J. E., Innes, K. K.: J. Mol. Spectr. **15**, 407 (1965)
15. McHugh, A. J., Gouterman, M.: Theoret. Chim. Acta (Berl.) **13**, 249 (1969)
16. Robin, M. B., Kuebler, N. A., Brundle, C. R.: In: Shirley, D. A. (Ed.): Electron spectroscopy, p. 370–373. Amsterdam, London: North-Holland Publishing Company, 1972
17. Fridh, C., Åsbrink, L., Lindholm, E.: Chem. Phys. Letters **15**, 282 (1972)
18. Shulman, J. M., Moskowitz, J. W.: J. Chem. Phys. **47**, 3491 (1967)
19. Innes, K. K., Byrne, J. P., Ross, I. G.: J. Mol. Spectr. **22**, 125 (1967)

20. Sponer, H., Rush, J.: J. Chem. Phys. **20**, 1847 (1952)
21. Al-Jobourg, M. I., Turner, D. W.: J. Chem. Soc. p. 4434 (1964)
22. Clementi, E.: J. Chem. Phys. **46**, 4725 (1967); **46**, 4731 (1967); **46**, 4737 (1967)
23. Picket *et al.*: J. Am. Chem. Soc. **75**, 1618 (1953)
24. Price, W. C., Walsh, A. D.: Proc. Roy. Soc. (Lond.) **179** A, 20 (1941)
25. Herzberg, G.: Electronic spectra of polyatomic molecules, New York: Van Nostrand, 1966
26. Turner, D. W.: Advances in physical organic chemistry **4**, 31 (1966)
27. Robinson, G. W., El-Sayed, M. A.: Mol. Phys. **4**, 273 (1961)
28. Brinen, J. S., Goodman, L.: J. Chem. Phys. **35**, 1219 (1961)
29. Fischer, G., Small, G. J.: unpublished
30. George, G. A., Morris, G. C.: J. Mol. Spectr. **26**, 67 (1968)
31. Hummel, R. L., Ruedenberg, K.: J. Phys. Chem. **66**, 2334 (1962)
32. Pariser, R.: J. Chem. Phys. **24**, 250 (1956)
33. Hammond, V. J., Price, W. C., Teegan, J. P., Walsh, A. D.: Discuss. Faraday Soc. **9**, 53 (1950)
34. Glass, R. W., Robertson, L. C., Merritt, J. A.: J. Chem. Phys. **53**, 3857 (1970)
35. Hochstrasser, R. M., Marzzocco, C.: J. Chem. Phys. **49**, 971 (1968)
36. Ellis, R. L., Kuehnlenz, G., Jaffé, H. H.: Theoret. Chim. Acta (Berl.) **26**, 131 (1972)
37. Hackmeyer, H., Whitten, J. L.: J. Chem. Phys. **54**, 3739 (1971)

Dr. M. Zerner
Assistant Professor
Dept. of Chemistry
University of Guelph
Guelph, Ontario, N1G 2W1
Canada